

CALCIUM MOLYBDATE, CaMoO_4 : A PROMISING TARGET MATERIAL FOR $^{99\text{m}}\text{Tc}$ AND ITS POTENTIAL APPLICATIONS IN NUCLEAR MEDICINE AND NUCLEAR WASTE DISPOSITION

E.V. Johnstone,^{1,2} K.R. Czerwinski,¹ T. Hartmann,³ F. Poineau,¹ D.J. Bailey,⁴ N.C. Hyatt,⁴ N. Mayordomo,⁵ A. Nuñez,⁶ F.Y. Tsang, A.P. Sattelberger,⁷ K.E. German,⁸ E. J. Mausolf^{1,2}

¹ University of Nevada – Las Vegas, Chemistry and Biochemistry Department, Las Vegas, NV, USA

² Global Medical Isotope Systems (GMIS), Las Vegas, NV, USA

³ University of Nevada – Las Vegas, Department of Mechanical Engineering, Las Vegas, NV, USA

⁴ University of Sheffield, Department of Materials Science and Engineering, Sheffield, UK

⁵ Helmholtz-Zentrum Dresden-Rossendorf, Institute of Resource Ecology, Dresden-Rossendorf, Germany

⁶ Centro de Investigaciones Energéticas. Medioambientales y Tecnológicas (CIEMAT), Madrid, Spain

⁷ Chemical Sciences and Engineering Division, Argonne National Laboratory, Lemont, IL, USA

⁸ A. N. Frumkin Institute of Physical Chemistry and Electrochemistry, Moscow, Russia

DOI: 10.13140/RG.2.2.31901.36328

Introduction

Calcium molybdate (CaMoO_4) is a robust, inorganic material known for its favorable physicochemical properties making it ideal for a wide scope of applications including optics (i.e., phosphors, scintillators, laser hosts, etc.) [1], nuclear waste encapsulation and disposal [2 – 5], corrosion inhibition [6], etc. Calcium molybdate occurs in nature as the mineral powellite, and the compound adopts the scheelite (CaWO_4) structure-type with Mo fully oxidized in the +6-oxidation state [7]. This Mo-containing mineral phase exhibits limited solubility in aqueous environments and relative thermal stability at elevated temperatures. In the laboratory, CaMoO_4 can be synthesized straightforwardly from the stoichiometric solid-state reaction of MoO_3 with the respective calcium oxide or carbonate, e.g., CaO or CaCO_3 , at elevated temperatures, or alternatively via co-precipitation, sol-gel, or mechanochemical methods [8 – 10]. Depending on synthetic conditions, single phase nano-powders to monoliths can be generated and tailored for its successive application. Likewise, the scheelite structure type can incorporate different doping elements into the host lattice, such as Pb^{2+} or elements arising from the lanthanoid series, which are used for phosphor applications [11-13].

On the periodic table, Mo ($Z = 42$) is located on the 5th row within the transition metals and precedes the lightest, inherently radioactive element, technetium (Tc , $Z = 43$) [14]. Molybdenum is characterized by an assortment of naturally occurring isotopes (i.e., ^{92}Mo 14.53%, ^{94}Mo 9.16%, ^{95}Mo 15.84%, ^{96}Mo 16.67%, ^{97}Mo 9.60%, ^{98}Mo 24.39%, and ^{100}Mo 9.82%) making it a suitable starting material for the transmutation to an array of different Tc isotopes depending on isotope enrichment, particle beam type (e.g., proton, deuteron, electron, neutron, photon, etc.), and beam energy. One of the most recognized Mo-Tc radionuclidic parent-daughter couples is ^{99}Mo - $^{99\text{m}}\text{Tc}$, where the daughter isotope $^{99\text{m}}\text{Tc}$ has been characterized as the workhorse of the nuclear diagnostic imaging industry used worldwide in 30 to 40 million procedures annually, i.e., ~ 9,000 6-day Ci at end of processing (EOP) per week [15]. As the international geopolitical attitude towards using highly enriched uranium (HEU) for the production of ^{99}Mo begins to shift, the use of non-fission sources for the production of $^{99\text{m}}\text{Tc}$ is becoming increasingly more attractive, and new methods for production and separation are desperately being sought. For example, the United States of America currently has no domestic supply in place for the production of $^{99\text{m}}\text{Tc}$, although it is responsible for half of the world's usage.

When considering both, the isotopic and physicochemical composition and properties of Mo and CaMoO_4 , strong arguments can be made to pursue the better understanding of CaMoO_4 and its relationship as a host material for direct transmutation of $\text{Mo} \rightarrow \text{Tc}$ and / or post-processing integration of Tc at the atomistic level to weight percentages in its fundamental structure. In this work, the synthesis and irradiation of CaMoO_4 using a modular, fusion-based neutron source and

its successive characterizations are reported. Further discussions are presented considering these empirical data and their context with potential applications in the realms of nuclear medicine and materials.

Materials and Methods

Synthesis and Characterization of CaMoO_4 . Equimolar mixtures of powdered MoO_3 (natural abundance of Mo isotopes) and CaO were intimately ground together as a slurry in ethanol with a mortar and pestle. The resulting powder was subdivided and pressed together as a green body pellet using an uniaxial press. The green bodies were reacted in a platinum-lined alumina crucible at 860°C for 6 hr in a furnace under flowing argon gas or normal atmosphere. The samples were then re-homogenized, pressed into pellets, and reacted for an additional 4 hr. The resulting pellets weighed approximately 3.1 g with a total sample size of CaMoO_4 for irradiation of ~ 12.1 g.

Powder X-ray diffraction (PXRD) was performed on the synthesized samples using a Bruker D8 Advance diffractometer employing $\text{Cu K}\alpha_1$ radiation. Representative areas from each puck were manually removed and ground with a mortar and pestle. The samples were blended with a silicon metal line standard and distributed on a low-background silicon wafer XRD sample holder. The samples were scanned in the region of 10 - 120° 2θ and analyzed using Topas 4.0 software.

Neutron irradiation of CaMoO_4 . The synthesized CaMoO_4 pellets were stacked within a 50 mL polypropylene centrifuge tube in between pieces of high-density polyethylene (HDPE), in so that they were located at the approximate center of the tube or roughly 12 cm from the neutron source while situated within the holder. The tube and its contents were placed in a HDPE cavity and situated adjacent to a neutron source. The point source had a neutron output of approximately 10^9 neutrons per second ($\sim 10^6$ neutrons $\cdot\text{cm}^{-2}\cdot\text{s}^{-1}$) with energies of 2.45 MeV at the origin of production, and the CaMoO_4 was irradiated for roughly 1.5 hr. Total neutron production over the irradiation period was $\sim 1.54 \times 10^{12}$ neutrons. Following end of bombardment (EOB) resulting ^{99}Mo - $^{99\text{m}}\text{Tc}$ activities were measured on a NaI gamma spectrometer for a count time of ~ 200 s; activities were corrected for decay incurred during transfer from the point source to the spectrometer after EOB. Information on detector efficiencies nor geometric positioning on the NaI detector have been provided, instead these values in a system of 100% capture efficiencies are assumed and used for correlating subsequent production rates.

Results and Discussion

Synthesis and Characterization of CaMoO_4

Calcium molybdate samples were synthesized using a method similar to that reported by Abdel-Rehim [8, 16]. This method yielded dense pucks that fluoresced under a UV light source as is shown in **Figure 1**. The effect of atmosphere on the synthesis of these materials was negligible as can be seen in **Figure 2**. When pulverized, the bulk material also fluoresced demonstrating an overall homogeneity within the monolith and formation of the intended compound. A quantity of these materials was removed and analyzed by PXRD. Analysis of the diffraction profiles indicated that some unreacted starting materials were still present in the sample (i.e., CaO), however, in relatively small amounts; these samples were reground with a mortar and pestle and reacted again at 860°C for 4 hr. In **Figure 3**, the CaMoO_4 samples and the irradiation container and configuration used for irradiation are presented.

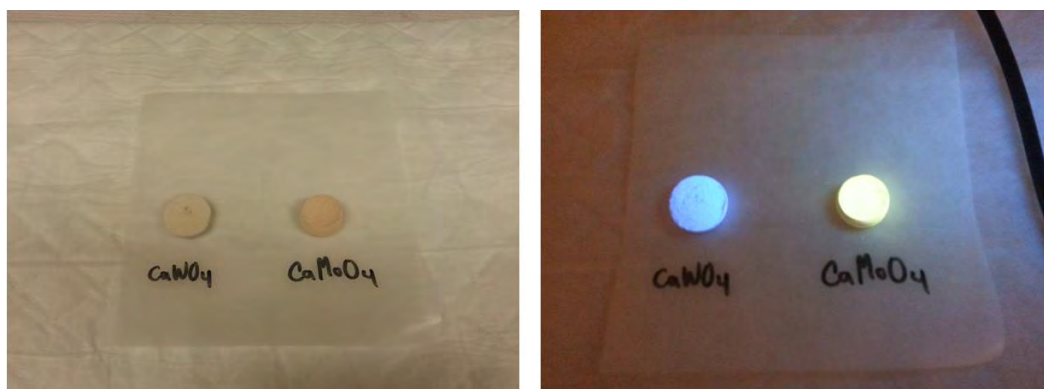


Figure 1. Synthetic scheelite (CaWO_4) and powellite (CaMoO_4) samples observed under ambient versus UV lighting showing fluorescent properties. Left: room lighting conditions. Left: UV lamp. Figure adapted from Ref. Ошибка! Закладка не определена..

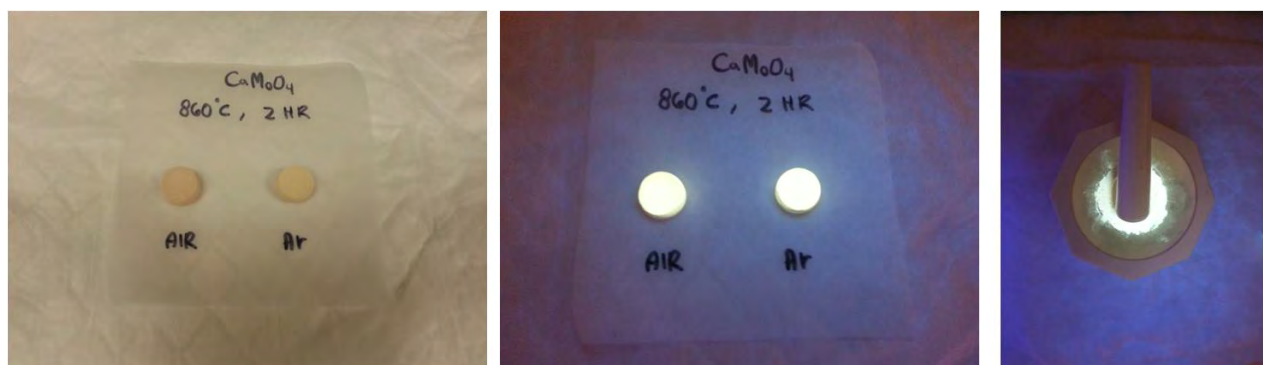


Figure 2. Comparison of synthetic powellite samples produced under an air or argon atmosphere at elevated temperatures. Left: room lighting conditions. Middle: UV light. Right: ground powder under UV lamp. Figure adapted from Ref.

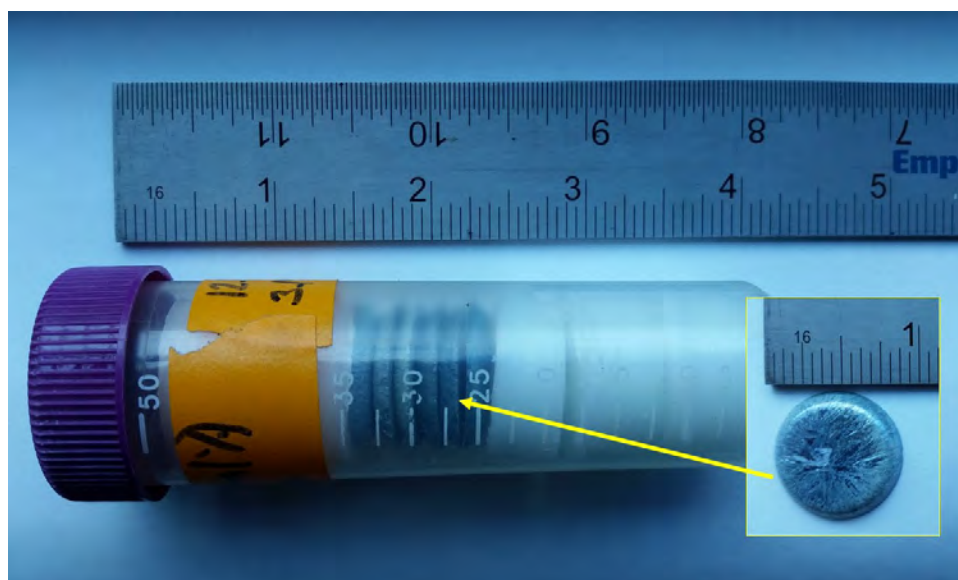


Figure 3. CaMoO_4 target material and irradiation containment used in this study. Ruler shown for scale. Inset: a representative pellet of CaMoO_4 .

Phase analysis and quantification of the bulk powder CaMoO_4 was performed by PXRD and subsequent Rietveld structure refinement, an example of which is shown in **Figure 4**. Results indicated that the composition of the bulk powder was CaMoO_4 with some unreacted starting materials, depending upon the sample. The CaMoO_4 was fit with the scheelite structure type with $I41/a$ symmetry (unit cell parameters of $a = 0.52266(4)$ nm and $c = 1.1435(1)$ nm) consistent with

previous studies [7]. Phase characterization of samples produced under an inert atmosphere yielded similar results (not presented here).

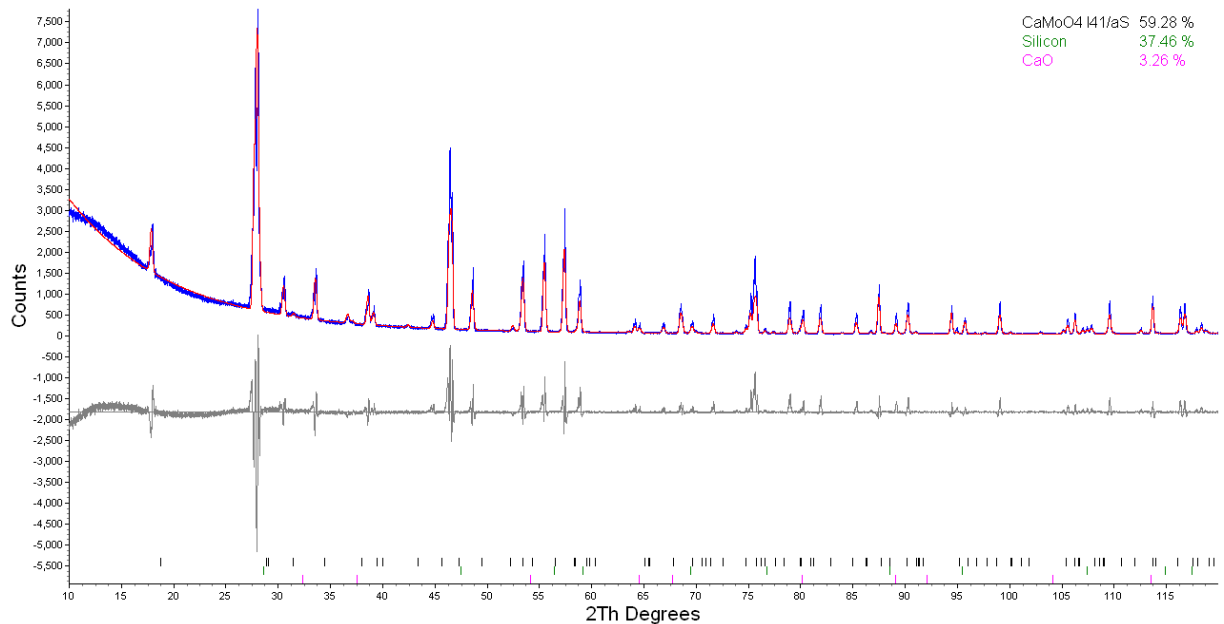


Figure 4. PXRD analysis of reaction products from MoO₃ and CaO at elevated temperature under air after 6 hours reaction time. Silicon is used as an internal standard. Figure adapted from Ref.

Neutron Irradiation of CaMoO₄ and ⁹⁹Mo-^{99m}Tc Production

The samples of CaMoO₄ and canister design were placed into a moderating block and irradiated adjacent to a neutron point source of $\sim 10^9$ n/s for 1.5 hr. The resulting samples were analyzed for activated products and more specifically for ⁹⁹Mo and ^{99m}Tc and the respective activity of each. In **Figure 5** and **Figure 6**, the gamma spectra of the irradiated samples are presented at different times after EOP.

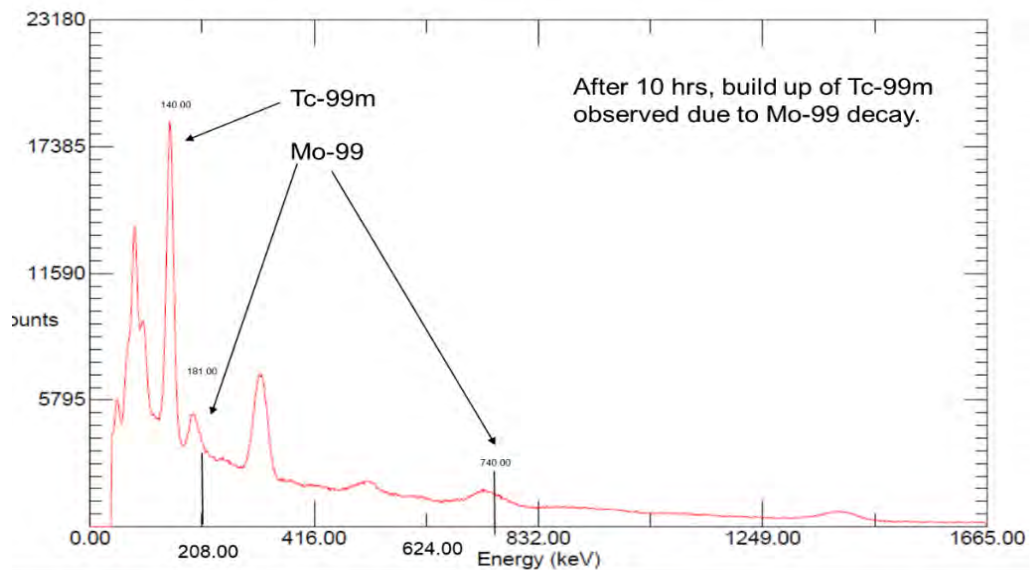


Figure 5. Gamma spectrograph of irradiated CaMoO₄ indicating ⁹⁹Mo and ^{99m}Tc measured 10 hr after EOP. Other unlabeled peaks are associated with unidentified, short-lived impurities in the matrix and background contributions, e.g., ⁴⁰K.

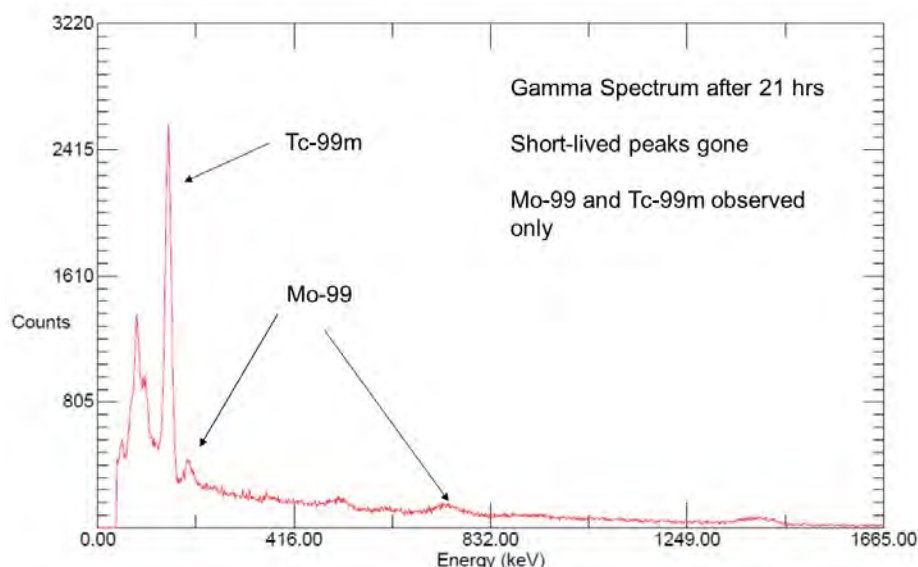


Figure 6. Gamma spectrograph of irradiated with identified ^{99}Mo and $^{99\text{m}}\text{Tc}$ approximately 21 hr after EOB. Other unlabeled peaks are associated with unidentified, short-lived impurities in the matrix and background contributions, e.g., ^{40}K .

Encapsulation and Immobilization of ^{99}Tc Nuclear Wastes

Technetium-99 is a long-lived ($t_{1/2} = 214,000$ yrs) nuclear byproduct of ^{235}U (~ 6% yield) fission, where it is found associated with the epsilon (ϵ) phase which contains, most notably, Mo-Tc-Ru-Rh-Pd. This metallic phase is highly resistant to corrosion, though Mo and Tc can be removed during nitric acid reprocessing activities [17]. Previous research has shown that these particles can be selectively separated using fluorine containing compounds in an inert atmosphere at elevated temperature [18]. They are difficult to recover due to their sub-nano radius and are found as colloidal inclusions that are removed by filtration and/or centrifugation after fuel dissolution. In direct-heated melter systems for waste glass fabrication, the formation of metallic globules can clog waste glass draining and the associated heat dissipation in the area of the bottom drain of the melter, resulting in lower melt temperature and higher viscosities. Due to the high melting point of these particles, methods such as plasma arc melting or induction techniques are required to process metallic billets greater than 10 g. These particles have also been shown to be associated with iodine (I) retention before uranium oxide, e.g., UO_2 , dissolution occurs. This result suggests that these compounds could play an important repository role in slowing the rate of both ^{99}Tc as pertechnetate ($[\text{TcO}_4]^-$) and ^{129}I as diatomic iodine (I_2) via the with interaction Ag and Pd nano-particles [19]. Tc is also problematic during glass melting processes where oxidizing conditions promote the formation of volatile Tc oxides and hydroxides that must be trapped in the off-gas scrubbing system and reprocessed back into a final waste form [20].

In nuclear spent fuel reprocessing, the spent fuel is dissolved in nitric acid and $[\text{TcO}_4]^-$ and uranyl ($[\text{UO}_2]^{2+}$) are co-extracted in tributylphosphate (TBP) (30 vol%) in dodecane or kerosene. Following extraction, Tc and U are both back-extracted into dilute nitric acid, and an anion exchange resin is used for the final separation of Tc from $[\text{UO}_2]^{2+}$. Thereafter, Tc is transformed into a robust material, such as metal / alloy or a glass, for final disposition [21]. The Closed End-to-End (CETE) demonstration was an exercise that applied the Uranium Extraction (UREX) process to yield mg quantities of Tc metal via hydrogen reduction post fuel dissolution. This Tc was eventually incorporated into stainless steel (SS-316)/Zirconium (Zr), SS-316 [Pd-Rh-Ru], and pure epsilon phases (Mo-Tc-Ru-Rh-Pd) [22]. These phases have been shown to be robust waste-forms for Tc and possibly I when fuel is stored via the “once-through cycle” after placed in a hypothesized geological long-term repository.

Particularly problematic is the highly soluble and mobile form of Tc, the pertechnetate anion $[\text{TcO}_4]^-$, which is a byproduct of reprocessing and nuclear medicine scenarios and a potential

hazard to the biosphere when released in an uncontrolled fashion. Methods to encapsulate soluble $[\text{TcO}_4]^-$ have been explored using large and / or bulky organics containing soft-base donor ligands, primarily comprised of carbon and nitrogen. Although this form is suitable for subsequent processing into metal, it is not feasible to process most legacy waste, nor low specific activity (LSA) ground state Tc wastes biologically rejected from patients undergoing $^{99\text{m}}\text{Tc}$ SPECT imaging via urine. Specifically for Tc, due to the cost and volume burdens of the waste, it does not seem economically viable to recover low activity ^{99}Tc from these patients; however, the introduction of an element, which only occurs in ultra-trace quantities naturally, into the environment is not advisable and should be avoided. Therefore, it is proposed that the co-precipitation of CaMoO_4 and $\text{Ca}(\text{TcO}_4)_2$ could be explored as a method to specifically encapsulate Tc into a glass, ceramic, or metallic waste form precursor across all waste classes.

It is expected that $\text{Ca}(\text{TcO}_4)_2 \cdot x\text{H}_2\text{O}$ would have a range of solubilities over a range of Ca concentrations – this is particularly important when considering charge balance in transmuted samples associated with $\text{Mo(VI)} \rightarrow \text{Tc(VII)}$ where a cationic excess would be present. Additionally, several $[\text{TcO}_4]^-$ salts with monocationic metals exhibit the scheelite-type structure and theoretically would be ideal for incorporation [22]; however, density functional theory (DFT) calculations have demonstrated that Tc would occupy the interstitial sites in the CaMoO_4 and CaWO_4 structures. To date, there is a significant gap in the literature associated with the solid-state synthesis of the mixed phases via co-precipitation of the compounds discussed in this paper.

Production and Separation of ^{99}Mo - $^{99\text{m}}\text{Tc}$.

The first (serendipitous) demonstration of using a Mo target for the production of Tc was the experiment performed via the international collaboration of American and Italian scientists Ernest Lawrence, Emilio Segre, and Carlos Perrier where molybdenum metal foil, a component of the Berkley cyclotron, was activated by the bombardment with a deuteron beam. Subsequent analysis of the radioactive Mo yielded the undiscovered, missing element $Z = 43$, which was later named technetium, alluding to the Greek word “τεχνητός” meaning “artificial” [23]. The use of Mo and Mo-containing targets for the production of ^{99}Mo - $^{99\text{m}}\text{Tc}$ specifically was later applied for the use in the emerging field of nuclear medicine and has since rapidly expanded with the development in detection methods, radiolabeling, etc. Whereas this was the original pathway for ^{99}Mo - $^{99\text{m}}\text{Tc}$ production in the first prototype generators, it was soon replaced by the use of highly enriched uranium (HEU) fission-based ^{99}Mo , which eventually became the “gold standard” for the radiopharmaceutical community. This change in direction was primarily driven by the fact that greater yields of ^{99}Mo could be produced with higher specific activities; processing and separation protocols were developed and have sustained the industry for several decades since this turn. However, the global community, reverting from the use of HEU, is actively pursuing alternative production methods for ^{99}Mo - $^{99\text{m}}\text{Tc}$, primarily the direct irradiation of Mo and Mo-containing target sources. Concerning this, there have been several production routes identified, typically dependent upon the particle beam utilized, e.g., photon, proton, deuteron, neutron, etc. and respective energy on either natural Mo, enriched ^{100}Mo or ^{98}Mo , or a combination of these. Particularly problematic with this route of production is the generation of LSA ^{99}Mo , which makes separation and radiolabeling increasingly difficult and inefficient with decreasing specific activity. To overcome this for the separation of the parent-daughter, various methods have been proposed where $^{99\text{m}}\text{Tc}$ in high specific activity (HSA) can be isolated from LSA ^{99}Mo target material. The technology options include liquid-liquid extraction (LLE) with methylethyl ketone (MEK), column chromatography with aqueous biphasic extraction chromatography (ABEC) or ion exchange (IE), chemical precipitation / gel generator, and thermal chromatographic separations [24, 25]. For the latter, thermal chromatographic separations were first demonstrated in the laboratory and in the clinical environment in Hungary [26]. This method has since been adopted and improved by scientists in Japan, where the problem of low(er) yields of $^{99\text{m}}\text{Tc}$ milking has been vastly improved [27]. Large enhancements in the process have involved: 1) the use of a MoO_3 target, in which the generated $^{99\text{m}}\text{Tc}$ is in its fully oxidized state in an oxygen-rich matrix allowing for the facile formation of volatile Tc oxides, and 2) complete sublimation of molten MoO_3 at

elevated temperatures ($\sim 840\text{ }^{\circ}\text{C}$) to overcome the low diffusion rates of transmuted $^{99\text{m}}\text{Tc}$ from the target. Other target materials for thermal separations that have also been investigated include molybdenum carbide Mo_2C and titanium molybdate [28, 29]. Some drawbacks observed for these techniques and materials have been associated with the regeneration of the Mo / Mo-containing target after thermal treatment, price of target production (enrichment increases costs significantly whether through HEU or Mo-enrichment), ease of target synthesis, and amount of Mo content available for transmutation.

In consideration to the results reported here, CaMoO_4 exhibits compositional stability at elevated temperatures under oxidizing environments and yields workable amounts of generated $^{99\text{m}}\text{Tc}$. Additionally, the range of synthetic routes, such as precipitation, high-temperature treatment, and mechanochemical formation, with an equally diverse possibility in material properties, like controlled nano-sized crystallization that have been reported in the literature, makes CaMoO_4 an ideal candidate as a Mo-containing material for $^{99\text{m}}\text{Tc}$ production coupled with thermal chromatographic separation techniques for use in the nuclear medicine industry, for example as a solid-state $^{99\text{m}}\text{Tc}$ generator following bombardment, though this is not yet known to be viable. The applicable use of this material has been evaluated and is provided in **Figure 7** for use as a $^{99\text{m}}\text{Tc}$ generator as it relates to the possible total ‘patient doses’ of $^{99\text{m}}\text{Tc}$ versus time of irradiation using neutron outputs ranging from 10^9 to 10^{15} n/s, where a ‘patient dose’ is defined as 20 mCi of $^{99\text{m}}\text{Tc}$ at time of use to a patient receiving a SPECT image. With approximately 40 million patient doses used annually worldwide, this is approximately 154,000 doses required daily, 5 days a week, 52 weeks a year. At EOB we correlate that over the course of the week, $\sim 400,000$ doses would be available, thus far exceeding the supply requirements of patients worldwide at the maximum neutron outputs of current day systems, i.e., reactors and spallation neutron sources. By exploiting a target of this nature, the market has room for expansion if the distribution chain does not contain the same inefficiencies of that observed from fission produced ^{99}Mo using HEU, i.e. decay losses are minimized due to decentralization of production and distribution. Therefore, natural samples bombarded within a reactor of decent neutron fluxes will generate similar patient doses.

In the heavier Tc homolog, rhenium (Re), several isotopes (^{186}Re and ^{188}Re) have been used for radiotherapeutic treatments. Unlike the ^{99}Mo - $^{99\text{m}}\text{Tc}$ couple, these isotopes are typically produced only from tungsten (W) or osmium (Os) targets, as neither of these Re isotopes nor their parent isotopes are generated in the fission process. Concerning this, literature has reported the cyclotron irradiation of mixed Mo-W and Mo-Os sulfide targets, i.e., MoS_2 , WS_2 , and OsS_2 , for the use as a Tc-Re generator for simultaneous radiotherapeutic-diagnostic treatments. Likewise, because of the scheelite solid-solution series with powellite and the similar volatile oxides formed for Tc and Re, i.e., M_2O_7 , HMO_4 , etc., mixed CaMoO_4 - CaWO_4 target materials could be used employing these thermal volatilization methods [31, 32].

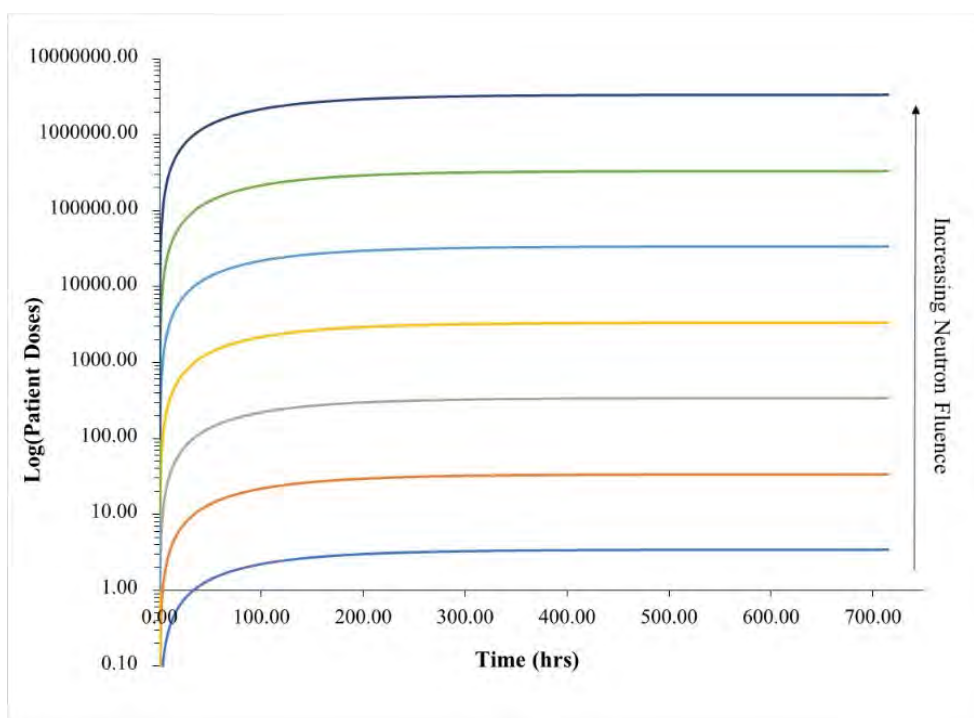


Figure 7. Predicted patient doses of ^{99m}Tc as a function of time and neutron source output (sequentially from 10^9 n/s (bottom blue) to 10^{15} n/s (top purple)) under ideal conditions as determined from activity measured within this study and proportionally scaled up to equivalent reactor fluences. One patient does of ^{99m}Tc is equivalent to 20 mCi.

Conclusions

The use of CaMoO_4 and some of its innate chemical and physical properties as a target material for the production of ^{99}Mo - ^{99m}Tc via neutron irradiation have been investigated. The material was synthesized using solid-state techniques, and upon neutron irradiation with a low-flux point source, both ^{99}Mo and ^{99m}Tc were observed in the target material post-irradiation by gamma spectrometry. With these results, the potential applications of CaMoO_4 and how they can be applied in various sectors of the nuclear industry, such waste encapsulation and disposal as well as the production of valuable radioactive isotopes for medical diagnostic and therapeutic procedures, were discussed. The authors believe that CaMoO_4 and similar powellite and scheelite materials have significant implications for application in commercial and industrial setting, especially those addressing the global shortage of ^{99m}Tc .

References

1. Thongtem, T.; Kungwankunakorn, S.; Kuntalue, B.; Phuruangrat, A.; Thongtem, S. "Luminescence and absorbance of highly crystalline CaMoO_4 , SrMoO_4 , CaWO_4 and SrWO_4 nanoparticles synthesized by co-precipitation method at room temperature," *J. Alloy. Comp.* **2010**, 506, pp. 475–481.
2. Kindness, A.; Lachowski, E. E.; Minocha, A. K.; Glasser, F. P. "Immobilisation and fixation of molybdenum (VI) by Portland cement," *Waste Manag.* **1994**, 14, pp. 97–102.
3. Taurines, T.; Boizot, B. "Synthesis of powellite-rich glasses for high level waste immobilization," *J. Non-Cryst. Sol.* **2011**, 357, pp. 2723 – 2725.
4. Bosbach, D.; Rabung, T.; Brandt, F.; Fanghänel, T. "Trivalent actinide coprecipitation with powellite (CaMoO_4): Secondary solid solution formation during HLW borosilicate-glass dissolution," *Radiochim. Acta.*, **2009**, 92, pp. 639—643.
5. Hand, R J.; Short, R. J.; Morgan, S.; Hyatt, N. C.; Möbus, G.; Lee, W. E., "Molybdenum in glasses containing vitrified nuclear waste," *Glass. Tech.* **2005**, 46, pp. 121—124.

6. Vukasovich, M. S.; Farr, J. P. G. "Molybdate in corrosion inhibition – A review," *Polyhedron*, **1986**, 5, pp. 551–559.
7. Senyshyn, A.; Kraus, H.; Mikhailik, V. B.; Vasylechko, L.; Knapp, M. "Thermal properties of CaMoO_4 : Lattice dynamics and synchrotron powder diffraction studies," *Phys. Rev. B*, **2006**, 73, pp. 014104-1 – 014104-9.
8. Abdel-Rehim, A. M. "Thermal analysis and X-ray diffraction of synthesis of powellite," *J. Therm. Anal. Calor.* **2001**, 64, pp. 1283–1296.
9. Pramanik, P. "A novel chemical route for the preparation of nanosized oxides, phosphates, vanadates, molybdates and tungstates using polymer precursors," *Bull. Mater. Sci.* **1999**, 22, pp. 335–339.
10. Hoseinpur, A.; Bezanaj, M. M.; Khaki, J. V. "Mechanochemical synthesis of CaMoO_4 nanoparticles: Kinetics and characterization," *Int. J. Mater. Res.* **2016**, 107, pp. 935–941.
11. Yang, P.; Yao, G.; Lin, J. "Photoluminescence and combustion synthesis of CaMoO_4 doped with Pb^{2+} ," *Inorg. Chem. Comm.*, **2004**, 7, pp. 389–391.
12. Dutta, P. S.; Khanna, A. " Eu^{3+} Activated Molybdate and Tungstate Based Red Phosphors with Charge Transfer Band in Blue Region," *ECS J. of Solid St. Sci. Tech.* **2013**, 2(2), R3153-R3167.
13. Schmdit, M.; Heck, S.; Bosbach, D.; Ganschow, S.; Walther, C.; Stumpf, T. "Characterization of powellite-based solid solution by site-selective time resolved laser fluorescence," *Dalton Trans.* **2013**, 42, pp. 8387–8393.
14. Johnstone, E. V.; Yates, M. A.; Poineau, F.; Sattelberger, A. P.; Czerwinski, K. R. "Technetium: The first radioelement on the Periodic Table," *J. Chem. Educ.* **2017**, 94, pp. 320–326.
15. OECD Nuclear Energy Agency, "The Supply of Medical Radioisotopes: 2017 Medical Isotope Supply Review: $^{99}\text{Mo}/^{99\text{m}}\text{Tc}$ Market Demand and Production Capacity Projection 2017-2022," *OECD*, **2017**, Paris, pp. 1–29.
16. Chernesky, W.; Johnstone, E.; Borjas, R.; Kerlin, W.; Ackerman, M.; Mayo, K.; Kim, E.; Poineau, F.; Czerwinski, K. R., "Development of fluorescent technetium compounds as a radioactive distributed source," *SDRD FY 2014 – Instruments, Detectors, and Sensors*, **2014**, RSLN-25-14, pp. 59–69.
17. Buck, E. C.; Mausolf, E. J.; McNamara, B. K.; Soderquist, C. Z.; Schwantes, J. M. "Nanostructure of metallic particles in light water reactor used nuclear fuel," *J. Nucl. Mater.*, **2015**, 461, pp. 236–243.
18. McNamara B. K.; Buck, E. C.; Soderquist, C. Z.; Smith, F. N.; Mausolf, E. J.; Scheele, R. D. "Separation of metallic residues from the dissolution of a high-burnup BWR fuel using nitrogen trifluoride," *J. Fluor. Chem.* **2014**, 162, pp. 1–8.
19. Buck E. C.; Mausolf, E. J.; McNamara, B. K.; Soderquist, C. Z.; Schwantes, J. M. "Sequestration of radioactive iodine in a silver-palladium phase in commercial spent nuclear fuel," *J. Nucl. Mater.*, **2016**, 482, pp. 229–235.
20. Childs, B. C., "Volatile technetium oxides: Implications for nuclear waste vitrification," *University of Nevada – Las Vegas Thesis*, **2017**.
21. Mausolf, E. J., "Separation of Tc from U and development of metallic Tc waste forms," *University of Nevada – Las Vegas Thesis*, **2013**.
22. Ackerman, M.; Kim, E.; Weck, P. F.; Chernesky, W.; Czerwinski, K. R., "Technetium incorporation in scheelite: insights from first-principles," *Dalt. Trans.* **2016**, 45, pp. 18171–18176.
23. Perrier, C.; Segrè, E. "Technetium: The element of atomic number 43," *Nature*, **1947**, 159, pp. 24.
24. Magdalena, G. "Separation methods of cyclotron-produced $^{99\text{m}}\text{Tc}$," *Nucl. Med. Bio.*, **2017**, 58, pp. 33–41.
25. Dash, A.; Knapp, F. F., Jr.; Pillai, M. R. A. " $^{99}\text{Mo}/^{99\text{m}}\text{Tc}$ separation: An assessment of technology options," *Nucl. Med. Bio.* **2013**, 40, pp. 167–176.

26. Gerse, J.; Kern, J.; Imre, J.; Zsinka, L. "Examination of a portable $^{99}\text{Mo}/^{99\text{m}}\text{Tc}$ isotope generator/SUBLITECH," *J. Radioanal. Nucl. Chem. Lett.* **1988**, *128*, pp. 71—80.
27. Nagai, Y.; Kawabata, M.; Sato, N.; Hashimoto, K.; Saeki, H.; Motoishi, S. "High thermo-separation efficiency of $^{99\text{m}}\text{Tc}$ from molten $^{100}\text{MoO}_3$ samples by repeated milking tests," *J. Phys. Soc. Jap.* **2014**, *83*, pp. 083201-1—083201-4
28. Richards, V. N.; Mebrahtu, E.; Lapi, S. E. "Cyclotron production of $^{99\text{m}}\text{Tc}$ using $^{100}\text{Mo}_2\text{C}$ targets," **2013**, *40*, pp. 939—945.
29. Zsinka, L.; Kern, J. "New, portable generator for the sublimation of technetium-99m," IAEA-CN-45/39 Report, 1988, pp. 95—106.
30. Gott, M. D.; Hayes, C. R.; Wycoff, D. E.; Balkin, E. R.; Smith, B. E.; Pauzauskie, P. J.; Fassbender, M. E.; Cutler, C. S.; Ketring, A. R.; Wilbur, D. S.; Jurisson, S. S. "Accelerator-based production of the $^{99\text{m}}\text{Tc}$ - ^{186}Re diagnostic-therapeutic pair using metal disulfide targets (MoS_2 , WS_2 , OsS_2)," *Appl. Rad. Iso.*, **2016**, *114*, pp. 159—166.
31. Fernandez-Gonzalez, A.; Andara, A.; Prieto, M. "Mixing properties and crystallization of the scheelite-powellite solid solution," *Cry. Grow. Des.*, **2007**, *7*, pp. 545—552.
32. Richards, V. N.; Rath, N.; Lapi, S. E., "Production and separation of $^{186\text{g}}\text{Re}$ from proton bombardment of ^{186}WC ," *Nucl. Med. Bio.*, **2015**, *42*, pp. 530—535.